Tube-Wall Catalytic Reactor Cooled by an Annular Heat Pipe

Cooling a tube-wall reactor using an annular heat pipe (*AHP*) is more temperature-stable, more flexible and more productive than cooling by conventional means. Tube-wall reactors cooled by an annular heat pipe arrangement exhibit flatter temperature profiles and uniform redistribution of the imposed heat load. The combination of tube-wall reactor and annular heat pipe is subject to the usual capacity limitations of the heat pipe: sonic flow, boiling heat transfer, liquid entrainment, and capillary flow of the working fluid.

Y. O. PARENT
W. R. Grace & Co.
Washington Research Center
Columbia, MD 21044

H. S. CARAM
Lehigh University
Bethlehem, PA 18015

R. W. COUGHLIN
University of Connecticut
Storrs, CT 06268

SCOPE

Selective hydrocarbon oxidation and several other industrial reactions require close temperature control to avoid complete oxidation that could destroy the desired product and possibly deactivate the catalyst being used. For such highly exothermic reactions, the heat transfer rate is a primary design consideration. The high heat transfer rates required by these reactions are usually achieved by using small-diameter reactor tubes in a shell-and-tube type of heat exchanger, or the use of fluidized-bed reactors with immersed heat exchange surfaces or transport-line reactors where the high heat capacity of the solid can maintain near-isothermal conditions. Tubular reactors are favored for selective exothermic reactions owing to their favorable residence-time distributions and their simplicity.

Some difficulties associated with tubular reactors are sharply-peaked axial temperature profiles ("hot spots") and great sensitivity to sudden adventitious changes in operating conditions that can produce large deleterious temperature excursions ("runaway conditions"). During operation with a "hot spot," only a small fraction of the catalyst is actually used, *viz.*, the catalyst in the vicinity of the temperature maximum. Flattening sharp temperature peaks can improve the catalyst utilization. To accomplish this, higher heat transfer rates must be achieved between the reacting surface and the cooling medium. To avoid quenching the reaction and to insure rapid rates and high productivity, coolants which can sustain high temperatures are often used. The tube-wall reactor employs a thin catalytic layer deposited on the reactor wall to reduce thermal resistance between the reacting surface and the cooling medium to a thin reactor wall and the liquid film on the coolant side.

Further improvement can be achieved by making the chemically reactive surface an integral part of the evaporator portion of a heat pipe. Thereby, the convective resistance of the coolant is replaced by a conduction resistance across the liquid-saturated wick of the heat pipe. The latter resistance can be several times less than the convective resistance of the previous system. The heat generated by chemical reaction vaporizes the working liquid of the heat pipe; the vapor thus generated flows to a cooled surface of much larger area where it condenses. This condensate flows from the cool condenser surface back to the hot evaporation region under the influence of capillary-pressure forces in the porous wick. This arrangement provides two notable thermal advantages: (1) extremely high local heat transfer coefficient at the evaporation surface, and (2) dilution of the large heat flux at the much more extensive condensing surface.

The heat transfer rate of the heat pipe may be limited, however, by any of the following: (1) rate of capillary flow in the wick, (2) boiling regime, (3) entrainment of the liquid from the wick into the flowing vapor, and (4) restriction or "choking" of the vapor flow rate in the internal spaces of the heat pipe.

In this paper the steady-state operation of a tube-wall reactor cooled by a liquid is compared with that of the same reactor cooled by an annular heat pipe. The advantages and limitations of the latter system are elucidated. Special utility and advantages are attained by designs which employ heat pipes of annular configuration surrounding a tube-wall reactor.

CONCLUSIONS AND SIGNIFICANCE

Selective oxidation of naphthalene to phthalic anhydride in a tube-wall reactor is improved by cooling with *AHP* as compared with an identical reactor conventionally cooled by liquid flow. The significant advantages derive from the ability of the heat pipe to maintain a more uniform axial temperature profile.

With cooling by the *AHP* ignition of the sequential parasitic reaction (oxidation of phthalic anhydride) is delayed and the reactor can be operated at higher temperature without a loss in yield of the desired product. It was also observed that a much shorter reactor can achieve 95–96% conversion while maintaining high yield of the desired product. Another marked improvement is the reduction of the sensitivity of the maximum wall temperature to upsets in temperature of the reactor or its feed; temperature "runaway" conditions are thus greatly attenuated. Finally, the restrictions on the temperature of the external coolant can be relaxed and operation with smaller coolant-side heat transfer coefficients becomes feasible.

Because higher reaction rates can be obtained using the AHP, the entire system benefits from a reduction in size, weight,

---

0001-1541-83-6876-0442-$2.00.

pressure drop requirements and a possible increase in productivity. More uniform catalyst temperature also extends the active life of the catalyst; in fact "hot spot" migration as the catalyst ages can actually produce a more uniform AHP heat load distribution and more favorable operating conditions.

Because final heat sink temperature and overall heat transfer coefficient can be lowered significantly, reactor designs can employ smaller heat fluxes and more conventional or practical cooling fluids (e.g., water or air instead of molten salts). The improvement is due to increases in both available heat transfer area and in the range of stable operational temperatures.

To avoid exceeding the operational limits of the heat pipe device, the special annular configuration considered requires several modifications to the usual design equations used for conventional axial heat pipes. These operating limits involve capillary flow of working fluid (as liquid) in the wick, sonic or choke flow of the working fluid (as vapor) in the vapor space, entrainment of liquid from the wick into the flowing vapor and boiling heat transfer to the working liquid; these phenomena are considered briefly. It is also shown that if any of these operating limits is exceeded for a given heat flux distribution it is possible to circumvent the difficulty by dividing the internal fluid-flow circuits of the heat pipe so that part of the hot working vapor is conducted in the upstream direction into a feed preheater section where it condenses.

HEAT PIPE DEVICE

The combination of a chemical reactor with a heat pipe has been proposed before by Basiulis and Plost (1975) who suggested the use of axial heat pipes in a heat-exchanger-type, tube-wall reactor for the methanation reaction. Later, Biery (1977) investigated the design of a fixed bed methanator in which axial heat pipes and columns of stacked cylindrical catalyst pellets formed a tightly packed array. Axial heat pipes can also be inserted directly into a heat-generating fixed or fluidized bed to enhance heat removal and assist in waste heat recovery. Incorporating a heat pipe device of annular configuration as an integral part of a chemical reactor has, to our knowledge, not been previously considered or analyzed.

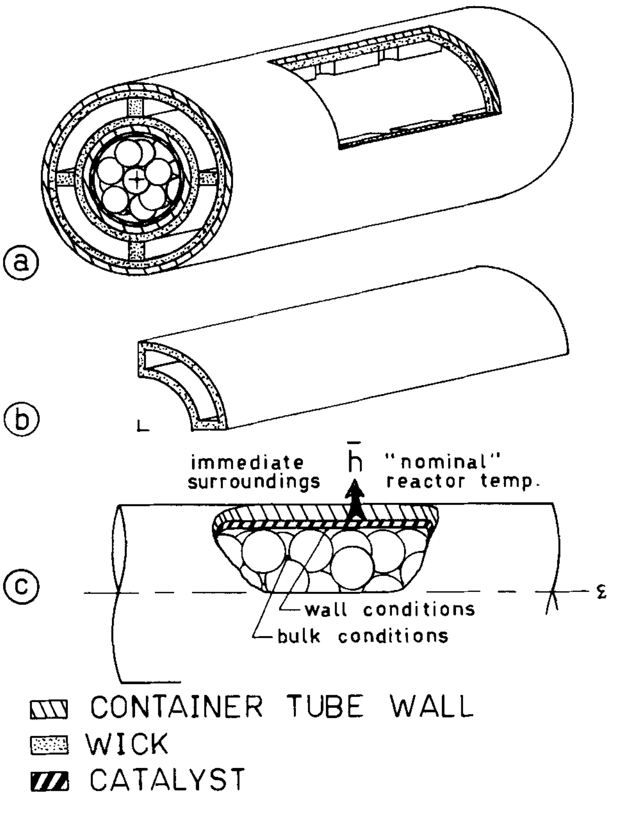

Figure 1. Reactor model: a. cutaway view of *AHP* reactor; b. basic *AHP* wick channel element; c. reactor tube model (packing is inert).

A heat pipe is a closed, static heat transfer device with high apparent thermal conductivity. Very large thermal fluxes driven by modest temperature gradients are achieved by the continuous circulation of a working fluid which vaporizes in the region where the device absorbs heat and condenses where heat is discharged.

The annular heat pipe device is constructed as a closed container formed by two coaxial tubes joined at both ends by annular disks. The surfaces of the tubes forming the closed annular cavity are lined with a porous material which serves as a wick for the liquid phase. The coaxial porous liners are connected by "spokes" of porous material. The wick assembly so formed operates saturated with the liquid phase of an appropriate working fluid (Figure 1a).

The operation of heat pipe devices is restricted by the occurrence of any one of four major physical limitations: 1. boiling of the liquid in the wick matrix, 2. entrainment of liquid droplets from the wick by the vapor, 3. choking of vapor flow (sonic limit), and 4. the insufficiency of the porous wick to return condensed liquid to the evaporator by capillary flow. These phenomena and conventional approaches to their analysis are discussed extensively in the literature (Chi, 1976; Bienert and Skrabek, 1972; Dunn and Reay, 1978).

Although detailed analysis of heat pipe operating limits for the annular configuration can be found elsewhere (Parent, 1980; Parent et al., 1981), here we rely upon only the function equations which express these individual limiting phenomena for the annular heat pipe. The maximum allowable heat flux $Q_{\max}$ across the device in steady-state operation may be set by any one of the previously mentioned phenomena. These limits will always depend on the heat load distribution $F(q)$ and the fluid properties and for each of them on the following additional physical quantities:

- Boiling limit: wick properties, maximum local flux $q_{\max}$
- Entrainment limit: wick properties, geometry of the annular space
- Choke or sonic limit: geometry of the annular space
- Capillary limit: wick properties, vapor flow regime, geometry of the annular space, vapor and liquid pressure distributions

The boiling, entrainment and sonic limits of the AHP are derived in a similar manner as for conventional axial heat pipes. The capillary liquid flow limit, however, requires a quantitative formulation of the bidimensional pressure distribution for flow which is imposed by a given heat flux distribution function $F(q)$ in the *AHP*. Previously mentioned references give a complete analysis of fluid flow in the wick of the annular heat pipe. If a heat pipe is operated beyond one of the physical limits, a sharp, continuous, localized temperature increase will be evident on the evaporator portion. Unless the device has suffered physical damage in the process, normal operation can be re-established upon cooling of the evaporator.

Chemical Reactor Application for Annular Heat Pipe

Oxidation of naphthalene in a tube-wall reactor has been the subject of considerable published analysis and design (Carberry, 1976; Smith and Carberry, 1975; Smith, 1970; Peters, 1967). The analysis given here is also for this reaction, but in a tube-wall reactor cooled by an annular heat pipe. This reaction system was chosen as an example, since it entails extreme conditions which require reactor-design considerations such as: multiple (parallel and series) reactions, high (exothermic) heat of reaction, conversion and yield restrictions, occurrence of "hot spots," thermal sensitivity, and a relatively high operating temperature range (~673 ± 50 K).

The reaction is usually carried out using fixed beds of catalyst in tubes cooled by a molten salt or similar fluid or by using a boiling liquid flowing in a shell which surrounds the tubes in a typical heat-exchanger configuration (Rase, 1977; Carberry, 1976; Smith and Carberry, 1975). Radial and axial temperature gradients are significant, and the system is susceptible to rapid temperature changes in the "hot spot" portion of the reactor. Heat and mass-transfer processes are found to be the limiting factors.

In recent years, the technology of depositing thin layers of catalytically active metals, oxides and alloys on metallic surfaces has led to the development of the tube-wall reactor (*TWR*) (Mills and Steffgen, 1973; Haynes et al., 1972; Gross et al., 1969; Peters, 1967). Smith and Carberry (1975) explored the application of the tube-wall reactor configuration to naphthalene oxidation for which they optimized the design. Their data and approach were used as points of departure for the present study in which cooling by an *AHP* replaced the "molten salt" convection cooling, although for the high heat transfer coefficient involved the comparison is also valid for the boiling liquid reactors.

The two systems (one with the *AHP* and the other with conventional cooling) were then compared using the simple one-dimensional reactor model discussed below. No effort was made to optimize the design of the *AHP* system.

The apparent advantage of the heat pipe is the low thermal resistance between the reactor internal surface and the essentially isothermal heat-pipe vapor space. The vapor in the vapor space, in turn, distributes the total heat load uniformly at the sink interface. By its configuration, the *AHP* provides increased heat transfer resulting in a "dilution" of the heat flux density. This should permit the use of a more conventional ultimate sink or final coolant.

The study was carried out in two parts: first, the reactor model was used to compare the behavior of the system with and without an operative *AHP* device. Secondly, the heat load distribution imposed by the reactor side of the AHP was tested to verify that the limits of the *AHP* (Parent, 1980; Parent et al., 1981) were not exceeded and that the device would indeed operate.

Kinetic and Reactor Models

The simplified kinetic model for the oxidation of naphthalene considered by Smith and Carberry (1975) is:

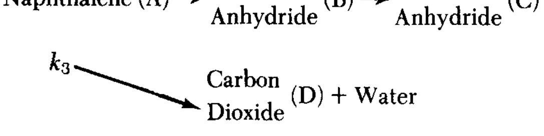

The desired product is phthalic anhydride (B) and each of the three rate processes (k_1, k_2, k_3) is considered to be irreversible and first order with respect to the concentration of the organic reactant. Figure 1c shows the reactor configuration; plug flow reactor operation is assumed. With reaction rates r_1, r_2 and r_3 expressed per unit of reactor wall area, the mass conservation equations for naphthalene (A), phthalic anhydride (B) and maleic anhydride (C) are:

$$\frac{d}{dz}X_A = \frac{M_w}{Gy_0}(r_1 + r_3) \tag{1}$$

$$\frac{d}{dz}Y_B = \frac{M_w}{Gy_0}(r_1 - r_2) \tag{2}$$

$$\frac{d}{dz}Y_C = \frac{M_w}{Gy_0}r_2 \tag{3}$$

X_A, Y_B and Y_C are related to the total molar flow rates by the equations:

$$X_A = \frac{N_{Ao} - N_A}{N_{Ao}};\ Y_B = \frac{N_B}{N_{Ao}};\ Y_C = \frac{N_C}{N_{Ao}}$$

The reaction rates used in Eqs. 1, 2 and 3 are written in term of wall concentrations, thereby accounting for the mass-transfer resistance between the wall and the bulk fluid. They are given by:

$$r_1 = k_1\left(\frac{4}{D_t}\right)C_{AW};\ C_{AW} = \frac{k_m y_0(1 - X_A)\,\rho_M}{(k_m + k_1 + k_3)}$$

$$r_2 = k_2\left(\frac{4}{D_t}\right)\left(\frac{y_0 Y_B \rho_M k_m + k_1 C_{AW}}{k_m + k_2}\right)$$

$$r_3 = k_3\left(\frac{4}{D_t}\right)C_{AW}$$

Because the heat of reaction is released at the catalytic wall the thermal energy balance for the bulk gas is:

$$C_p\frac{dT_G}{dz} = \left(\frac{M_w}{Gy_0}\right)\frac{4\bar{h}}{D_t}(T_W - T_G) \tag{4}$$

Equating the rate of heat generation at the catalytic wall to the rate of heat removal gives an algebraic expression for the wall temperature

$$T_W = \frac{\bar{h}_W T_G + \bar{h}T_R + \frac{D_t}{4}\sum_{j=1}^{3} r_j(-\Delta H_j)}{\bar{h}_W + \bar{h}} \tag{5}$$

The foregoing formulation disregards axial heat conduction with the result that estimates of temperature maxima will be conservative. As will be noted below, however, this treatment predicts temperature profiles which have some peculiarities ascribable to neglect of axial heat conduction. The following momentum conservation equation (Tallmadge, 1970) is used to obtain the pressure distribution.

$$\frac{dP_G}{dz} = -10^{-6}\frac{\rho_M M_w V_S^2(1 - \epsilon_b)\,M^*}{d_p\epsilon_b^3} \times \left\{\frac{150\,(1 - \epsilon_b)\,M^*}{Re_S} + 4.2\left(\frac{1 - \epsilon_b}{Re_S}\right)^{1/6}\right\} \tag{6}$$

where

$$M^* = 1 + \frac{2d_p}{3\,(1 - \epsilon_b)\,D_t}$$

Further assumptions in the analysis are: ideal behavior of the gas, constancy of the average molecular weight of the mixture and uniform bulk temperature in the transverse direction.

Equations 1, 2, 3, 4, and 6 can be numerically integrated using the following initial conditions: $T_G = T_{\text{feed}}$, $P_G = P_{\text{feed}}$, $T_W = T_{Wo}$ (obtained from Eq. 5 by iteration). Boundary conditions at $z = 0$ are $X_A = Y_B = Y_C = 0$.

Criteria for Comparison

The same reactor model is used for both the conventional liquid-cooled reactor and the *AHP* system. The distinguishing feature, however, is the mode and rate of heat transfer from the reactive surface. In the conventional case heat transfer is between reactive surface and a liquid coolant; in the case of the *AHP*, heat transfer is from reactive surface to the vaporizing working fluid in the wick. When a conventional liquid coolant is used, it is assumed to be at a uniform "nominal" reactor temperature; in this case $\bar{h}$ is the overall heat transfer coefficient between the reactive wall and the liquid, with most of the thermal resistance concentrated in the liquid film. In the case of the *AHP* system however the only resistances found between the reactive surface and the vapor space

TABLE 1. DATA FOR *AHP* REACTOR STUDY

Initial Values

$X_A = 0; Y_B = Y_C = 0$

$T_{FEED} = 523\ K \rightarrow 823\ K$; by increments of 100 K

$T_S = 533\ K \rightarrow 793\ K$; by increments of 10 K

$P_{G\ FEED} = 481.3$ kPa

$P_{G\ EFFLUENT} \geqslant 101.3$ kPa

Physical, Geometrical & Design Parameters

$G = 8.0\ kg/m^2{\cdot}s$ $\Delta H_1 = 1.6 \times 10^6\ J/mol$ (exothermic)
$y_o = 0.09$ $\Delta H_2 = 1.5 \times 10^6\ J/mol$ (exothermic)
$C_p = 29.98\ J/mol{\cdot}K$ $\Delta H_3 = 4.64 \times 10^6\ J/mol$ (exothermic)
$d_p = 3.0 \times 10^{-3}\ m$ $\bar{h}_c = 3.55 \times 10^3\ W/m^2{\cdot}K$
$D_t = 1.0 \times 10^{-2}\ m$(I.D.) $\bar{h}_{AHP} = 1.105 \times 10^4\ W/m^2{\cdot}K$
$\epsilon_b = 0.47$

AHP Geometry and Materials

Heat transfer fluid: Na or K

Wick material: stainless steel screens, 200 mesh

$w_t = 1.25 \times 10^{-3}\ m$ $R_{IN} = 1.0 \times 10^{-2}\ m$
$t_w = 2.0 \times 10^{-3}\ m$ $R_{OUT} = 2.09 \times 10^{-2}\ m$
$z_t = 3.0\ m$

of the *AHP* at the "nominal" temperature are those of the tube wall and the liquid-saturated metallic wick. A much higher value of $\bar{h}$ is thus expected in the case of the *AHP* cooled reactor. In the *AHP* case the reaction heat must ultimately be transferred from the *AHP* vapor to a suitable sink, the coupled behavior in which the final sink is included, is considered further below.

Values for $\bar{h}$ when a liquid coolant is used ($\bar{h}_c$) were estimated using the design procedure proposed by Kays and London (1964); they compared well with values calculated from the data provided by Smith and Carberry 1975. In the case of the AHP reactor, the value of $\bar{h}_{AHP}$ was found using the combined thermal resistance of the tube wall and of the saturated wick at an average temperature of 723 K. Pertinent data for these designs are given in Table 1. The equations of the reactor model were solved numerically using Lehigh University's Computer Center Library program DSS/2. A modified Runge-Kutta (Version #8 in DDS/2) integration algorithm was used with a relative error parameter set at 10^{-4}.

RESULTS OF THE COMPUTATION

The response of each configuration (with and without *AHP*) to changes in the inlet gas temperature and changes in the operating (nominal) reactor temperature (T_R) was investigated over the ranges specified in Table 1. Information provided by each simulation included: axial distributions of temperature and composition, the total heat generated by reaction, total conversion of (A), and yields of (B) and (C) in the reactor effluent, the maximum yield of (B) and the corresponding conversion of (A), and the axial position where maximum yield of (B) occurred.

The composition and temperature profiles generated by the conventional model without *AHP* were similar to those reported by Smith and Carberry (1975). For the inlet gas pressure employed, the maximum operating temperature of about 793 K was set by the pressure drop required for flow through the reactor. Beyond this stage reactor pressure drop would exceed the inlet pressure. A summary of the most important results follows.

Delayed Reaction Ignition

The superior heat transfer provided by the AHP system retards the "ignition" of the second series reaction (B → C). Figure 2 shows this effect as an enhancement in the curvature and a shift of the midsection of the double "S" heat generation curve when the *AHP* is substituted for conventional cooling. The lateral displacement of the second "ignition" step indicates that the ultimate sink can operate with lower heat transfer coefficients at lower temperatures to achieve the same risk of instability. Heat removal would be represented on Figure 2 by a straight line originating on the abcissa at the temperature of the ultimate sink; with the *AHP* this line need not have as steep a slope in order to give what is expected to be a stable operating point (crossing point with heat generation curve) in the neighborhood of the desired reactor temperature (723–748 K).

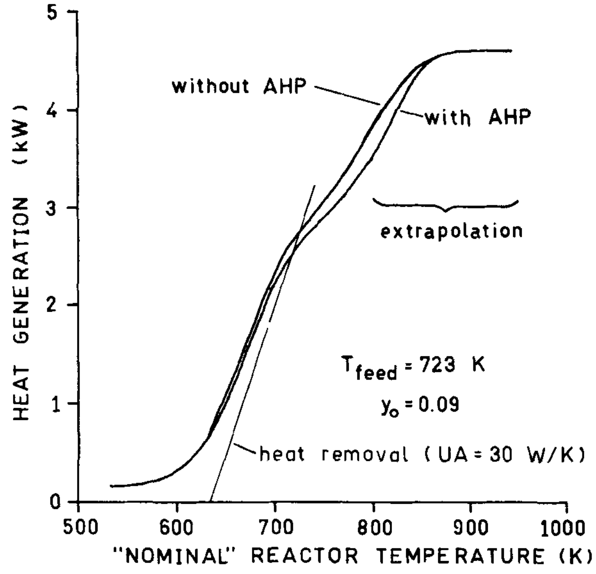

Figure 2. Heat generation curves.

Effluent Compositions and Maximum Yield of B

For the operating conditions under consideration, use of the AHP has little effect on the effluent composition or on the maximum yield obtainable in a 3.0-m reactor. Figure 3 shows only slight differences between the maximum yield of (B) obtainable in the effluent of either systems. The effect of better heat transfer is to reduce consumption of (B) that can otherwise occur when the conversion of (A) is increased by raising the temperature beyond that which produces optimum yield of (B). Commercial reactors ordinarily operate at conversions of naphthalene greater than 98.5%. Figure 4 compares the conversions of (A) and the corresponding maximum yields of (B) as a function of temperature and reactor length for the conventional reactor and for the *AHP*-cooled reactor. Neither the maximum yield of (B) nor the corresponding conversion of (A) are influenced by feed temperature. The dotted lines on Figure 4 show that the *AHP* reactor operating at ~760 K

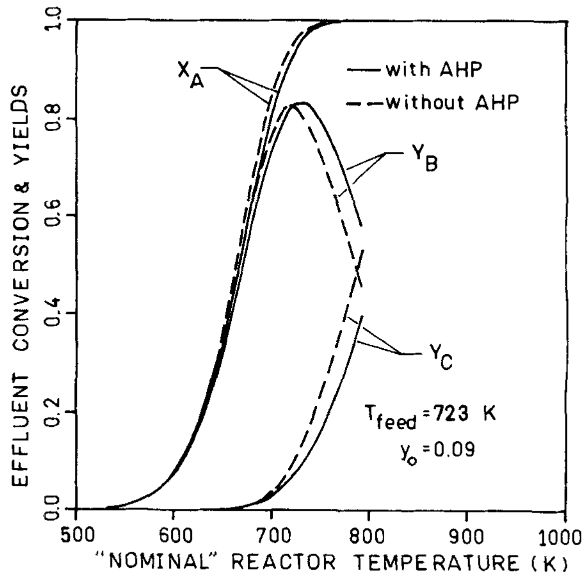

Figure 3. Effluent composition: reactor length, 3 m.

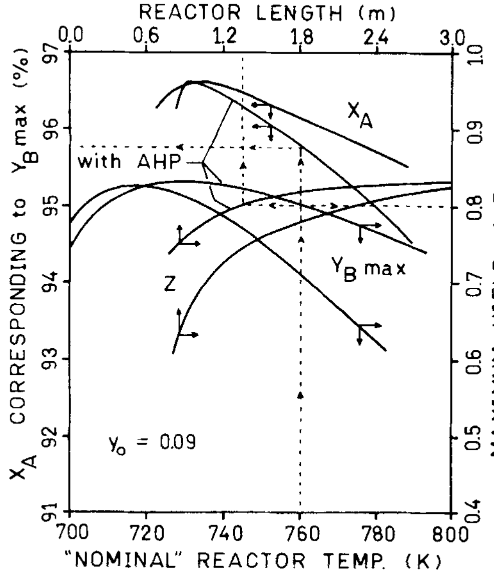

Figure 4. Maximum yield of (B) with corresponding position of occurrence and conversion of (A).

can produce a yield of (B) of ~80%, a conversion of reactant (A) of ~96% and require an active reactor length of 1.35 m. The system without *AHP*, for the same yield in (B) operates at a lower temperature (~735 K), gives a slightly higher conversion of (A) but requires a considerably greater length of 2.25 m. More important, and as evident from the graph, the system with the *AHP* will maintain a high yield of (B) for large range of operating temperatures in contrast with the conventionally cooled system in which Y_B falls far more steeply as the temperature rises. As seen, a noticeable decrease in reactor length can be achieved by operating at a higher temperature with the *AHP*. This can be done while maintaining X_A about 95% but without excessive loss in yield of (B) as has been shown.

Maximum Reactor Wall Temperature

Excessive excursions of the maximum wall temperature beyond the reactor temperature can occur for relatively small variations in the latter. This behavior is due to the onset of the second oxidation reaction. The better heat transfer provided by the *AHP* can diminish such temperature excursions and greatly reduce system sensitivity as shown in Figure 5 by curves 4A and 4B. With AHP the second oxidation reaction appears to become significant only at a higher sink temperature (~750 K) in contrast to the conventionally cooled system which begins to show excessive temperature rise from the second reaction at about 680 K. An important feature of the reactor behavior also shown in Figure 5, for example in curves 4A and 4B, is the occurrence of a crossing of the curves corresponding to different feed temperatures. The crossing results from the planar representation of a family of curves of a three variable function. We are indeed dealing with an "S" shaped folded surface for which accentuation in the folds increases as the feed temperature is lowered. The lower the feed temperature, the higher the temperature jump observed (so called "wrong-way" behavior). A detailed study of the sudden changes in maximum wall temperature is complicated by the existence of multiple solutions of the algebraic equations relating the wall temperature to the surrounding conditions. Moreover, axial heat transfer in the conductive wall of the reactor has been ignored in the present simulation thereby further limiting accurate quantitative estimation. For lower feed temperatures (523–623 K) the system exhibited multiple solutions in a limited range of operating reactor temperature (~650 to ~730 K). Although not shown here these results provide a definite qualitative indication of the sensitivity of the system to variations in feed and reactor temperature.

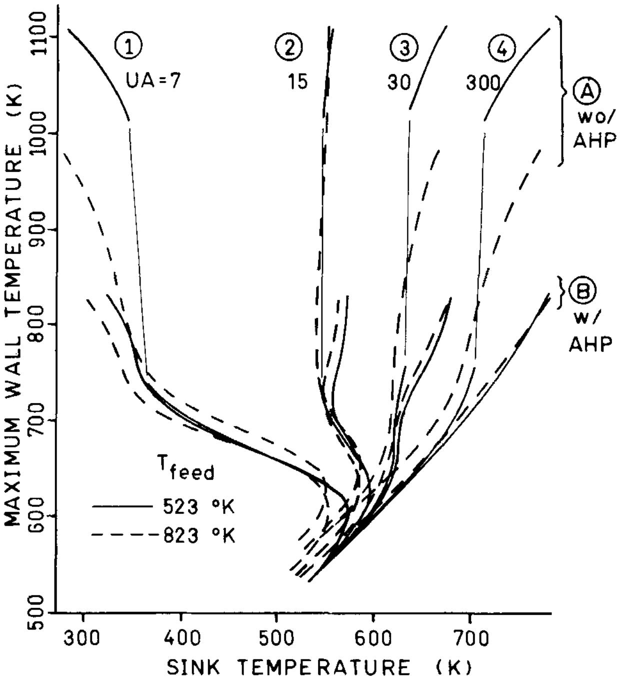

Figure 5. Final sink coupling (with and without *AHP*). *UA:* heat transfer rate/*K* between immediate surroundings and final sink. Curves: 1. *UA* = 7, 2. *UA* = 15, 3. *UA* = 30, 4. *UA* = 300; *UA* = W·m^2/m^2·*K*, y_o = 0.09.

The calculations presented so far accounted only for the effect of heat transfer between the reactor and its immediate surroundings (coolant flow or *AHP* vapor space). In practice, heat from either the *AHP* vapor space or from the liquid coolant must be transferred to a final sink (at temperature T_S) through a thermal resistance ($1/UA$). The effect of these two factors on the maximum reactor wall temperature is also shown in Figure 5. Each point on these curves represents a steady state condition corresponding to the given values of sink temperature, overall heat transfer coefficient and feed temperature. For the lower values of *UA*, some curves exhibit reversals in the sign of their slope, and thus multiple solutions for a given sink temperature. The positions of the reversal correspond to the "ignition points." Portions of the curves exhibiting negative slopes represent probably unstable points of operation for which slight perturbations will result in either a rapid temperature rise or quenching of the reactor. As discussed before, some of the curves corresponding to different feed temperatures show multiple crossings that can be interpreted as reactor instability when a decrease in the feed temperature corresponds to an increase in the maximum reactor temperature.

Comparing the group of curves A and B in Figure 5 shows that for the higher transfer rates ($UA > 30$), the *AHP* system extends noticeably the range of apparent stable operation by diminishing the sensitivity of maximum wall temperature to the final sink temperature. Under such conditions for the reactor without *AHP*, a sudden small increase in sink temperature could produce a very large and unacceptable excursion of wall temperature. Also important is the obvious capacity of the *AHP* system to operate stably at lower heat-transfer rates ($UA = 30$) while still allowing significant sink-temperature fluctuations without correspondingly great variations in maximum wall-temperature responses. Consider the case of the family of curves for which *UA* equals 15 (Figure 5); although there is a reversal in the slope, there exists a stable operating range which would *still* allow small variations in the sink temperature near 600 K. This is definitely not the case for the system without *AHP* which exhibits an unlimited excursion under comparable conditions. Finally, very low heat transfer rates ($UA < 15$) are unacceptable for either system since the only stable operating conditions correspond to quenched reaction temperatures or complete combustion of all of the products. In general, we can then say that the *AHP* system tends to lower the magnitude of the temperature excursion (hot spot) and broadens the acceptable range

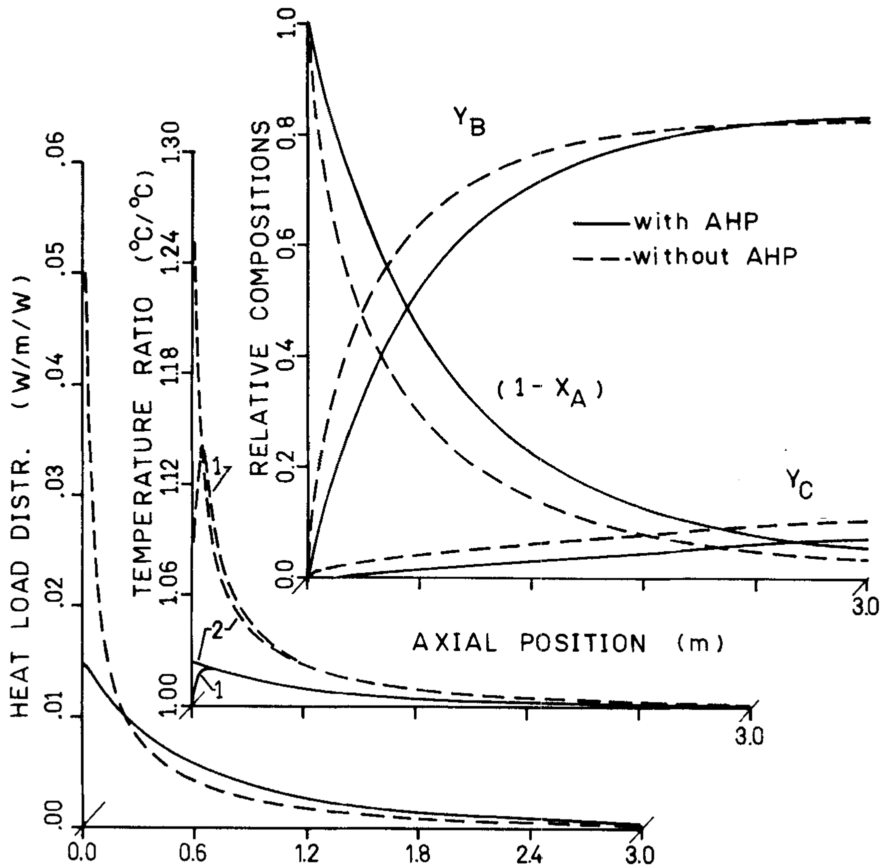

Figure 6. Axial Heat generation, temperature and composition profiles for: feed temp. = 723 K, nominal reactor temp. = 723 K, y_o = 0.09. Curves: 1. ratio of gas temp. to feed temp., 2. ratio of wall temp. to nominal reactor temp.

of final sink temperature fluctuations which do not upset stability.

Axial Profiles of Composition, Temperature and Heat Load

These are plotted in Figure 6 for a reactor-operating temperature of 723 K with a feed temperature of 723 K. The contrast between conventional cooling and the *AHP* system is evident and provides a fair basis of comparison between the two systems under these conditions. Although the system without *AHP* gives the best yield of B, the *AHP* system yields less undesired product (C) by slowing down the reaction process in the initial portion of the reactor. More importantly the *AHP*-cooled reactor exhibits a much flatter temperature profile and thereby permits a closer approach to isothermal operation. In the *AHP* system, the maximum reactor-wall

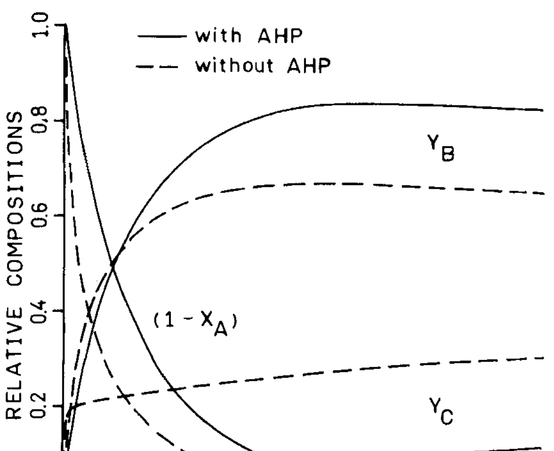

Figure 7. Axial composition profiles for: feed temp. = 723 K, nominal reactor temp. = 723 K, y_o = 0.135.

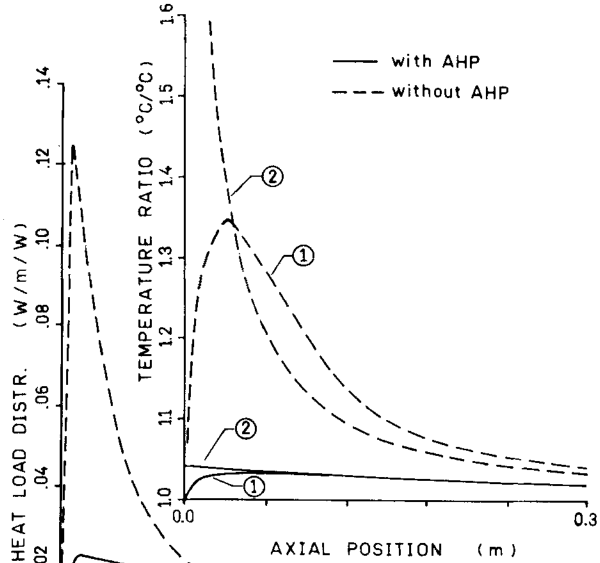

Figure 8. Axial heat generation and temperature profiles for: feed temp. = 723 K, nominal reactor temp. = 723 K, y_o = 0.135.

temperature rise is insignificant, corresponding to ~7% of the rise which occurs in the system without *AHP*. Also of major importance in the heat-transfer design of any reactor is the heat-load distribution profile which is also shown in Figure 6. The AHP system has a substantially more uniform distribution with a maximum heat flux, about 4 to 5 times less than with the other system.

Effect of Changes in Feed Composition

Figures 7 and 8 show the effects of an increase in the composition of reactant (A) in the inlet stream. Here the mole fraction of naphthalene in the feed is 0.135, compared to a value of 0.09 for the previously given results. With the higher feed composition the conventional system exhibits unacceptable yields and wall temperature while the AHP system shows little change in performance compared to operation with the feed of lower composition. Further increases in the reactant feed concentration does not cause drastic or unacceptable changes on the operations or behavior until mol fractions of naphthalene are equal or greater than 0.270. In those conditions there is a sudden take-off of the maximum of the heat load distribution and temperature together with a sharp drop in the selectivity. The AHP system also shows tolerance, although to a lesser extent, to change in tube diameter and mass flux. None of these characteristics are shown here.

DESIGN CONSIDERATIONS FOR THE *AHP*

Once the temperatures and heat loads have been obtained using the model described above, it is necessary to confirm that the *AHP* will indeed operate under those conditions. This entails verifying that none of the operating limits for the *AHP* is being exceeded by the proposed heat loads. Numerous geometrical configurations of an *AHP* can be so investigated. In the simplest design the entire outer cylindrical surface of the *AHP* contacts the surrounding heat sink and the inner cylindrical surface of the *AHP* is the reactor wall coated with catalyst.

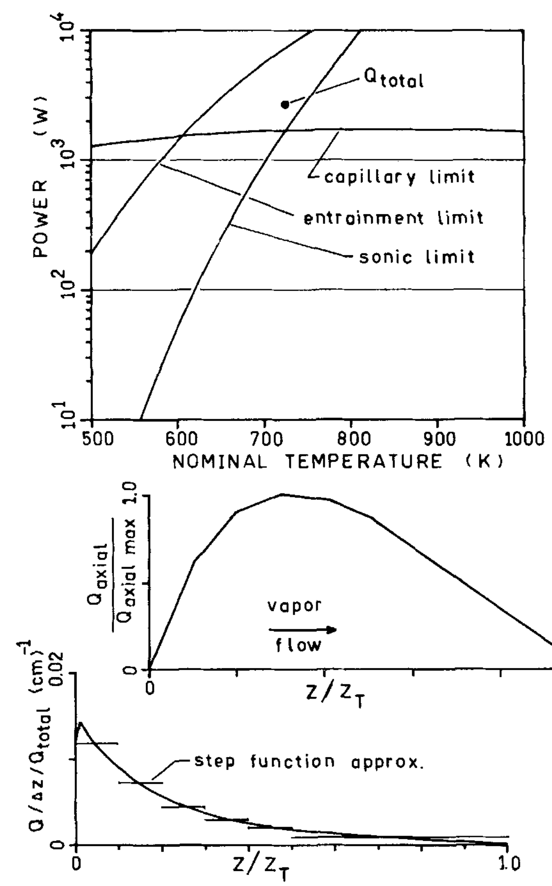

Figure 9. Predicted operating diagram, dimensionless axial heat flow profile and heat generation profile for the original *AHP* reactor model. Specifications; fluid Na, wick: 316 SS screens, 200 mesh, t_w = 0.002 m, z_T = 3 m, R_{IN} = 0.0062 m, R_{OUT} = 0.021 m, 4 rows of spokes, Q_{total} = 2578 W.

In the detailed analysis of the annular heat pipe presented elsewhere (Parent, 1980; Parent et al., 1981), axisymmetric heat load distributions are assumed thereby reducing consideration to a simplified wick structure as depicted in Figure 1b. Although the flow of working fluid in this crescent-shaped channel (liquid in the wick, vapor in the core) characterizes the performance of the device and governs its operational limits, computations require also that the axial heat load distribution be approximated by some suitable function. A simple approach is to represent an actual heat load distribution by a series of appropriate step functions. Unless the heat load is distributed uniformly on both inner and outer cylindrical heat-transfer areas, a net flow of working fluid will occur in the axial direction. It is this flow which determines the operating limits for each process involving the working fluid, with the exception of the boiling limit.

Figure 9 shows various operating limits for an *AHP* subject to a heat-load distribution as described in a design previously reported (Parent, 1980). The actual heat flow generated by the *AHP* reactor system (~2.6 kW) exceeds the operating limits for both sonic velocity of the vapor and capillary flow of liquid in the wick. This design is then inadequate. Figure 9 also shows the heat generation profile (with its step function approximation) which was used in the computation; the idealized axial heat (or vapor) flow profile is also given in Figure 9. These results refer to only one fluid-flow circuit.

To remove the limitations evident in Figure 9 both the capillary-flow limit and the sonic flow limit must be increased if the heat flux distribution given is to be achieved. The capillary limit can be increased by changing the heat transfer fluid or the wick material. The sonic limit can be improved by increasing the outer tube radius, by changing the heat transfer fluid or by raising the tem-

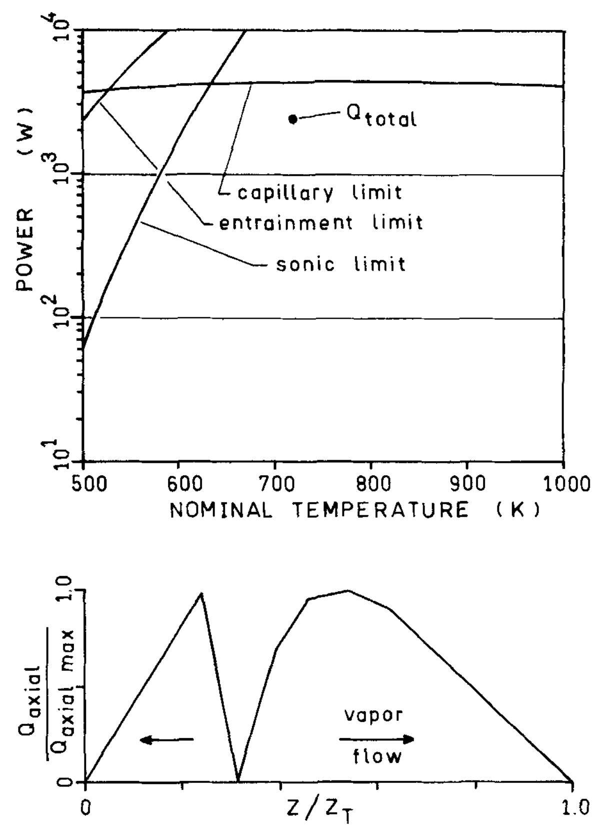

Figure 10. Predicted operating diagram and dimensionless axial heat flow profiles for the *AHP* reactor model with added entrance section (preheater). Specifications: fluid, *K*; wick, 316 SS sintered powder; t_w = 0.0012 m; z_T = 4 m; R_{IN} = 0.0062 m; R_{OUT} = 0.021 m; 4 rows of spokes, Q_{total} = 2,578 W.

perature of operation. Each of these alternatives were successfully tried with the exception of expanding the tube diameter.

In order to lower the ratio Z_T/D_t another heat flux distribution was investigated. Because most of the heat is generated in a narrow region at the beginning of the reactor it is possible to remove the limiting conditions by adding a section at the reactor entrance where working fluid condenses. This increases the overall length of the system but serves as a feed preheater. The effect is to create a different pattern of flow of the working fluid to accommodate a higher heat load. In this flow pattern, working fluid vaporized at the reactor entrance flows as a vapor into the upstream preheater where it condenses the wick conducts the condensed working liquid back to the evaporation zone. As an example, an acceptable design can be obtained in this way using potassium as the heat transfer fluid and an additional one meter condenser section at the beginning of the reactor. The corresponding operating diagram is given in Figure 10 together with the axial heat (vapor) flow profile resulting from this different design.

DISCUSSION

The hypotheses and assumptions used to determine the operational limits of the annular heat pipe have been published elsewhere (Dunn and Reay, 1978; Chi, 1976; Bienert and Skrabek, 1972). The isothermicity of the *AHP* vapor space is a reasonable assumption as long as the operation of the device is far removed from choke flow conditions (sonic limit).

The analysis (Parent, 1980) for which results were given above was developed for wicks of homogeneous porous material lining the container wall. Other types of wick are possible; for example, a composite wick might have a layer of lower flow resistance (larger pores) closest to the container wall contiguous to a second external layer with small pores that would provide the capillary pumping requirements.

Design optimization and heat pipe control were not considered in this study. Optimization should consider most favorable geometrical relationships among wick thickness, inner and outer tube radii, number of spoke rows and length for a particular working fluid, given materials of construction, and given axial heat-load distribution. Heat pipe control, although complex has been developed for axial heat pipes (Chi, 1976). For specific applications, self-control can be achieved by incorporating a noncondensable gas. Closed loop external control with a regulated heat sink or source also finds some applications in *AHP* devices.

The tube wall reactor seems to be the ideal application of the annular heat pipe, owing to the intimate contact of the relative wall with the porous wick. Nevertheless, fluidized-bed or fixed-bed reactors could also be cooled by the *AHP* although the major heat transfer resistance in a fixed bed reactor is often in the bed itself.

It has been assumed in the treatment above that heat transfer between the reactor tube wall and the isothermal vapor space was by radial conduction only. Actually, axial conduction can also contribute significantly and cause a further flattening of axial temperature profiles. Radiation heat transfer has been neglected in this analysis but its contribution would be an interesting subject for future investigation, especially at high temperatures. The simplified development given here suggests that the annular heat pipe reactor appears feasible, at least for a single tube device. Large-scale application could be limited further by economic considerations not investigated here.

NOTATION

AHP = annular heat pipe
C_i = concentration of component (i), mol/m^3
C_{iW} = concentration of component (i) at reactor wall, mol/m^3
CP = heat capacity of reaction mixture (average), J/mol·K
d = total derivative
d_p = diameter of inert reactor packing particles, m
D_t = inside diameter of reactor tube, m
$F(q)$ = heat flux distribution function across *AHP* heat exchange surfaces
G = mass flux of reactor feed stream, kg/m^2·s
$\bar{h}$ = heat transfer coefficient between inside reactor, and immediate surroundings J/m^2·s·K
$\bar{h}_{AHP}$ = heat transfer coefficient ($\bar{h}$) for the *AHP* reactor, J/m^2·s·K
$\bar{h}_c$ = heat transfer coefficient ($\bar{h}$) for the fluid flow reactor, J/m^2·s·K
$\bar{h}_W$ = heat transfer coefficient between gas and tube wall, J/m^2·s·K
ΔHj = heat released by reaction (j), J/mol
k_j = rate constant for reaction (j), m/s
k_m = mass transfer coefficient between gas and reactor wall, m/g
M_w = average molecular weight of gas mixtures, kg/kmol
N_i = number of moles of component (i), mol
P = pressure of gas mixture, kPa
q = heat flux, W/m^2
Q = heat flow, W
r_j = reaction rate of reaction (j), mol/m^3·s
$R_{\rm IN}$, $R_{\rm OUT}$ = inner most and outer most radii of *AHP* wick structure, m
Re_S = Reynolds Number based on superficial velocity
t_w = *AHP* wick thickness, m
T = temperature, K
TWR = tube-wall reactor
UA = heat transfer conductance, W/K
V_s = superficial velocity, m/s
w_t = tube-wall thickness, m
X_A = conversion of component (A)
y_o = mole fraction of reactant (A) in feed mixture
Y_i = yield of component (i)
z = axial coordinate
z_T = overall axial length, m

Greek Letters

ϵ_b = porosity of inert packed bed
ρ_M = molar density of gas feed, mol/m^3

Subscripts

G = gas
R = nominal reactor or immediate surroundings
S = sink
W = wall
o = initial
max = maximum or limit

LITERATURE CITED

Basiulis, A., and M. Plost, "Waste Heat Utilization Through the Use of Heat Pipe," ASME, No. 75-WA/HT-48 (Nov., 1975).

Bienert, W. B., and E. A. Skrabek, "Heat Pipe Design Handbook," Parts I-II, NASA-CR-134264, -134265 (Aug., 1972).

Biery, J. C., "Methanation with High Thermodynamic Efficiency Energy Recovery," Los Alamos Scientific Lab., LA-6656-MS (Jan., 1977).

Carberry, J. J., "Chemical and Catalytic Reaction Engineering," McGraw-Hill (1976).

Chi, S. W., "Heat Pipe Theory and Practice," McGraw-Hill (1976).

Dunn, P. D., and D. A. Reay, "Heat Pipes," 2nd ed., Pergamon Press (1972).

Gross, B., B. Grycz, and K. Miklossy, "Plasma Technology," American Elsevier (1969).

Haynes, W. P., J. J. Elliott, and A. J. Forney, "Experience with Methanation Catalysts," Preprint, Div. Pet. Chem., Amer. Chem. Soc., **16**, 2 (1972).

Kays, W. M., and A. L. London, "Compact Heat Exchangers," 2nd ed., McGraw-Hill (1964).

Mills, A. A., and F. W. Steffgen, "Catalytic Methanation," *Catalysis Reviews*, 8, 2, (159–210) (1973).

Parent, Y., "The Annular Heat Pipe Operating Limit Equations and Chemical Reactor Application," Ph.D. Thesis, Lehigh University (1980).

Parent, Y. O., R. W. Coughlin and H. S. Caram, "Operational Limits for the Annular Heat Pipe," in preparation.

Peters, H., "Catalytic Reactor Tube Liner," U. S. Patent 3,353,923, (1967).

Rase, H. F., "Chemical Reactor Design for Process Plants," **1–2**, Wiley (1977).

Smith, J. M., "Chemical Engineering Kinetics," 2nd ed., McGraw-Hill (1970).

Smith, T. G., and J. J. Carberry, "Design and Optimization of a Tube-Wall Reactor," *Chem. Eng. Sci.*, 30, 2, (221–227) (1975).

Tallmadge, J. A., "Packed Bed Pressure Drop—An Extension to Higher Reynolds Numbers," *AIChE J.*, **16**, 1092 (1970).

Manuscript received April 27, 1981; revision received February 23, and accepted June 18, 1982.

Combustion of Carbon Residue from Oil Shale Retorting

The combustion of a bed of particles impregnated with carbon is considered. An analysis is developed for the combustion wave after it has progressed some distance into the bed. It is shown that the calculations are considerably simplified by choosing a coordinate system that moves with the combustion wave and by neglecting dispersion of heat or mass.

MILTIADIS HISKAKIS and T. J. HANRATTY

Department of Chemical Engineering
University of Illinois
Urbana, IL 61801

SCOPE

In the combustion retorting of oil shale, a combustion wave is caused to move down through a bed of raw shale particles. Hot inert gases flow ahead of the wave and decompose the kerogen in the raw shale. Oil produced by this pyrolysis reaction is carried from the hot zone as a vapor, which condenses on cold shale particles and falls out the bottom of the bed as a liquid product. The pyrolysis of the kerogen leaves behind a carbon residue which provides the fuel for the combustion. The size of the oil yield from the process depends on keeping the combustion zone separated from the retorting zone and on minimizing the combustion of oil by oxygen which has bypassed the hot carbon residue.

We have been exploring a model of this process which solves the balance and rate equations in a coordinate system which moves with the combustion zone. Considerable simplifications of the equations are realized by neglecting dispersion of heat and mass in the flow direction and by assuming an adiabatic process. Our first step in implementing this model has been to consider the combustion of a bed of particles impregnated with carbon.

For large enough times, the combustion wave in a bed of burning carbon can reach a fully developed condition where the velocity, the temperature and the composition profiles do not change with time. This paper presents an analysis of this fully developed zone.

CONCLUSIONS AND SIGNIFICANCE

A modification of the general theoretical model of Baer and Dahl (1980) is used. In their analysis it is assumed that one percent of the oxygen in the inlet gas escapes unburned and that all of the carbon is consumed. It is shown that this assumption is not correct. In fact the calculation of the conversion of oxygen or of carbon emerges as the principle theoretical problem. Methods for calculating the effect of operating variables on the breakthrough of oxygen or of carbon are developed.

The errors involved in neglecting the influence of the dispersion of heat and of oxygen are explored. It is shown that these effects can be neglected provided the heat transfer coefficient between the gas and the solid is adjusted.

INTRODUCTION

The analysis uses separate heat balance equations for the gas and the solid and a shrinking core model for the carbon combustion. A parameter

$$\beta = \frac{\frac{\dot{m}_g}{A} C_g}{V \rho_s C_s (1-\epsilon)} \text{ is critically important.}$$

The condition $\beta \neq 1$ is necessary for the existence of a fully developed temperature wave (Baer and Dahl, 1980).

For $\beta < 1$, the combustion occurs at the front of the thermal wave that moves through the bed. The tail of the wave is an un-

---

M. Hiskakis is a fellow of the Alexandros Onassis Institute.

0001-1541-83-6440-0450-$2.00.